Sustainable Cities and Society 97 (2023) 104768

Contents lists available at ScienceDirect

Sustainable Cities and Society

journal homepage: www.elsevier.com/locate/scs

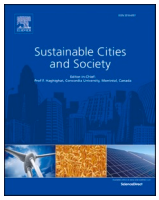

Using satellite imagery to investigate Blue-Green Infrastructure establishment time for urban cooling

L. Gobatti [a,b,*], P.M. Bach [a,b], A. Scheidegger [a], J.P. Leitão [a]

[a] Swiss Federal Institute of Aquatic Science & Technology (Eawag), Überlandstrasse 133, Dübendorf, ZH 8600, Switzerland
[b] Institute of Environmental Engineering, ETH Zürich, Zürich, ZH 8093, Switzerland

ARTICLE INFO

Keywords:
Blue-Green Infrastructure (BGI)
Nature-based solutions
Cooling establishment time (CET)
Land surface temperature
Normalized difference vegetation index (NDVI)
Urban heat mitigation

ABSTRACT

The process of urbanization can alter the local climate to the point that it threatens citizens' well-being by creating heat-related hazards. The construction of Blue-Green Infrastructure (BGI) can improve the regulation of surface energy exchange processes and address this problem. However, the time needed for a BGI to deliver a stable cooling performance, referred to here as the Cooling Establishment Time (CET), is poorly understood and quantified in the literature and dependent on environmental, design and maintenance factors. Here, we analyze the feasibility of using satellite data to derive the CET for different BGIs across the city of Zurich, Switzerland. Results showed that remote sensing can quantify the land surface temperature impact of BGIs and assist in estimating their CET. BGI with trees or climbing plants required a longer CET (seven to ten years) before any notable shift in surface temperatures were visible, while grasses or artificial irrigated systems led to shorter CETs (one to three years). These results allow us to better account for BGI cooling establishment when planning for areas that need urgent action under warming climates. This work supports evidence-based urban greenery planning and design towards cooling our increasingly warming cities in a timely manner.

1. Introduction

The process of urbanization increases heat absorption and storage by means of converting natural surfaces into human-built materials with higher solar energy absorption, lower albedo and greater thermal capacity and mass (Kaloustian & Diab, 2015; Bartasaghi Koc et al., 2018). As a consequence of the land-use change caused by urbanization, the overall vegetation amount and thus the cooling provided by them decreases (Jamei et al., 2019; Santamouris, 2013, 2016). This results in a phenomenon widely referred to as the Urban Heat Island (UHI) first reported by Howard (1818), which occurs when urban areas have a higher temperature than their surrounding rural areas (Rizwan et al., 2008; Oke et al., 2017; Aflaki et al., 2017; Deilami et al., 2018). A similar effect, but which takes into account the land surface temperature (LST) is the SUHI, or Surface Urban Heat Island, which is when urban areas have higher surface temperatures than their surrounding rural areas (Oke et al., 2017). The UHI and SUHI become more frequent as of global warming, and the number of extreme heat events have also been increasing (US EPA, 2016; IPCC, 2022). This combination of the urban heat islands with extreme climatic events can create scenarios where human well-being across city districts can be negatively affected (Back et al., 2021; Deilami et al., 2018).

To improve pedestrian-level thermal comfort and decrease heat exposure, there are two main approaches that can offer timely and cost-effective solutions: (i) increasing solar reflectance (Akbari & Kolokotsa, 2016; Santamouris et al., 2011; Santamouris, 2013); and (ii) increasing the amount of urban greenery through the implementation of Blue-Green Infrastructure (BGI), also known as Blue-Green Systems or Nature-based Solutions (Antoszewski et al., 2020; Probst et al., 2022; Zhou et al., 2017; Grilo et al., 2020).

BGIs are multi-functional networks of vegetation that can also comprise water bodies, including not only engineered systems but also natural landscape features (Probst et al., 2022; Sörensen et al. 2016; Ghofrani et al. 2017; Oral et al. 2020). As summarized by Probst et al. (2022), BGIs can reduce the UHI intensity by means of regulating the surface energy exchange process via evapotranspiration, reduction of short-wave radiation (Kim & Guldmann, 2014), emissivity regulation, heat dispersixffon and influencing air movement and heat exchange (Antoszewski et al., 2020), reducing convective and radiative heat fluxes (Jamei et al., 2020). However, it is not the goal of a BGI to influence the climate of the city as a whole, but rather contribute to small changes in the local microclimate.

* Corresponding author at: Swiss Federal Institute of Aquatic Science & Technology (Eawag), Überlandstrasse 133, Dübendorf, ZH 8600, Switzerland.
E-mail address: lucas.gobatti@eawag.ch (L. Gobatti).

https://doi.org/10.1016/j.scs.2023.104768
Received 24 March 2023; Received in revised form 30 June 2023; Accepted 30 June 2023
Available online 1 July 2023

A number of previous studies (e.g., Antoszewski et al., 2020; Deilami et al., 2018) have investigated the factors influencing the local LST or local air temperature reduction performance of BGIs, associating it to geometrical, surrounding built environment, morphological and vegetation parameters. Another group of studies focused in evaluating the establishment of vegetation: Monberg et al. (2019) measured species richness and composition before and after the implementation of a BGI; Fehmi and Kong (2012) investigated plant establishment and growth during revegetation processes, showing that site-specific conditions have large influence on plant establishment; Leinster (2006) and Mazer et al. (2011) indicated in very practical terms the establishment of a BGI vegetation, suggesting different construction and operation processes to guarantee that the system greenery will consolidate. Other group of studies mainly focused on monitoring the cooling performance of BGIs, such as Yang et al. (2022) who created a generic vegetation cooling efficiency index to evaluate urban vegetation cooling efficiency under different forcing conditions.

However, the cooling capacity is also time dependent as the construction of a BGI is often proceeded by a period of establishment (e.g., vegetation growth, root system establishment) such that it can deliver its expected benefits (Leinster, 2006). From the lens of thermal performance, we define here the term *Cooling Establishment Time* (CET) as the necessary time to reach a steady LST reduction performance starting from just after the end of the BGI construction.

To monitor cooling through time, satellite imagery was used by various studies, such as Maimaitiyiming et al. (2014), who investigated the relationship between LST and the configuration of green spaces, and Bartasaghi-Koc et al. (2019) who proposed a green infrastructure typology classification based on vegetation morphology and land-surface use within the BGIs. Satellite imagery offers the potential to evaluate large areas of space along a large time span, with enough time and space resolution for monitoring cooling performance changes within BGI with large areas (Hami et al., 2019). Although the spatial constrains are well defined, little has been done to explore the dynamics of these BGIs through time. Within this scope, there is a lack of understanding especially about the establishment time required for BGIs to achieve a stable cooling potential. Addressing this gap is necessary in order to not only improve our understanding of the cooling performance and the establishment of BGIs through time, but also to understand how this performance is associated with environmental and design aspects. Establishment time is taken into account in fields of Urban Stormwater Management on public BGI civil construction (Leinster, 2006) and Landscape Design (Nagase & Dunnett, 2013) with a view to create enough protection time to the system so it does not get destroyed by users or smothered by pollutants. This concept should also apply to cooling, given that there must be enough time taken into account so that the root system establishes for better substrate moisture uptake as well as for vegetation aerial parts to consolidate for more active evaporative cooling.

The objective of this study is to assess the feasibility of using open-source remote sensing data to identify the surface temperature changes associated with the implementation of BGI in urban areas and quantify their CET. To achieve these objectives, we monitored how LST at the BGI construction site changed over time relative to its surroundings and relative to its vegetation development. This is relevant when planning BGIs to tackle heat-related hazards, given that decision-makers and urban planners need more practical guidance on heat mitigation strategies (Bartesaghi Koc et al., 2018; Bartesaghi-Koc et al., 2020; Bowler et al., 2010) and need to be able to estimate the time required for BGIs to reach its expected cooling mitigation performance.

2. Materials and methods

To derive the necessary data from the BGI case studies, two different satellite pixels were observed: (i) the focal pixel that corresponds to the satellite image pixel that represents the land-use change from a gray area to a BGI; and (ii) the reference pixel that corresponds to a satellite imagery pixel that has not undergone land-use changes within the observation period. The proposed methodology is presented in Fig. 1. The different steps of the methodology, will be presented in detail in the next sections, describing the choice of case studies, the sources for satellite data as well as the steps to retrieve the net relative LST time series and estimate the CET for each BGI site.

2.1. Study area and selection of case study sites

We retrieved the LST time series within the footprints of six case studies located in the city of Zurich in Switzerland. The city of Zurich, according to the Köppen-Geiger climate classification is located within the Cfa boundaries (Beck et al., 2018): a temperate climate without dry season and with a hot summer. The different characteristics of each one of the case studies are presented in Table 1, including land use before and after BGI construction, construction period and approximate BGI area. Fig. 2 illustrates these land use changes and spatially references for each case study. The six case studies were selected based on their footprint area, given the spatial resolution limitations of satellite imagery (Bartasaghi-Koc et al., 2020), and also based on the construction year due to the limited time availability of the satellite imagery.

2.2. Data sources and computational resources

Each newly built BGI involves the addition of vegetation, and the more developed and established this vegetation is, the better should the BGI performance towards cooling be. The Normalized Difference Vegetation Index (NDVI) characterizes vegetation health and is also a proxy to the overall greenery development. It is a dynamic index which changes through time and will be derived for each case study. NDVI values range between -1 and $+1$, the smaller the value indicating unhealthier or sparse vegetation and the larger the value healthier or denser vegetation (Vina et al., 2011; Nouri et al., 2017; Dutta et al., 2015). Common values for extremely arid regions are NDVI $< +0.15$ (Eastman et al., 2013); for urban non-vegetated areas values are normally found at NDVI $< +0.20$; common thresholds for low urban vegetation are $+0.20 \leq$ NDVI $\leq +0.50$ and for high urban vegetation are $+0.50 <$ NDVI $\leq +1$ (Hashim et al., 2019). These values are considered for complete green coverage, not for scattered vegetation. It is relevant to highlight, however, that monitoring temperature using satellite imagery in this case only yields LST changes, and more specifically surface temperature changes happening in the top of the urban canopy layer as seen by the satellite's point of view. On top of that, LST reductions resulting from NDVI increases might not be fully accurate, given that the satellite will mostly capture the temperatures from the top of the vegetation instead from the shadowed areas that may have been created by this vegetation.

The National Aeronautics and Space Administration (NASA) Landsat 5 and 8 missions offer products for LST and NDVI, which attributes are presented in Table 2. These two satellite imagery products were chosen as the databases of this study, given the large temporal coverage that the combination of these datasets can provide, ranging from 1984 to the present date. A subset of these data was used in this research, ranging from 1985 (the first year when data are available all year round) to 2021. This allowed us to collect data from a large period before and after the construction of the BGIs. The year of 2012 was a gap due to the lack of reliable Landsat data.

Within satellite imagery products their spatial and time resolution are normally a trade-off: if it produces a finer spatial resolution the time resolution is coarser and vice-versa. The decision for using Landsat products also relates with their imagery having a pixel size of 30 m. Among the freely available satellite sources, this is a moderate spatial resolution, however it stills maintains a temporal resolution good enough for our goals.

To retrieve these data, which is within large datasets demanding

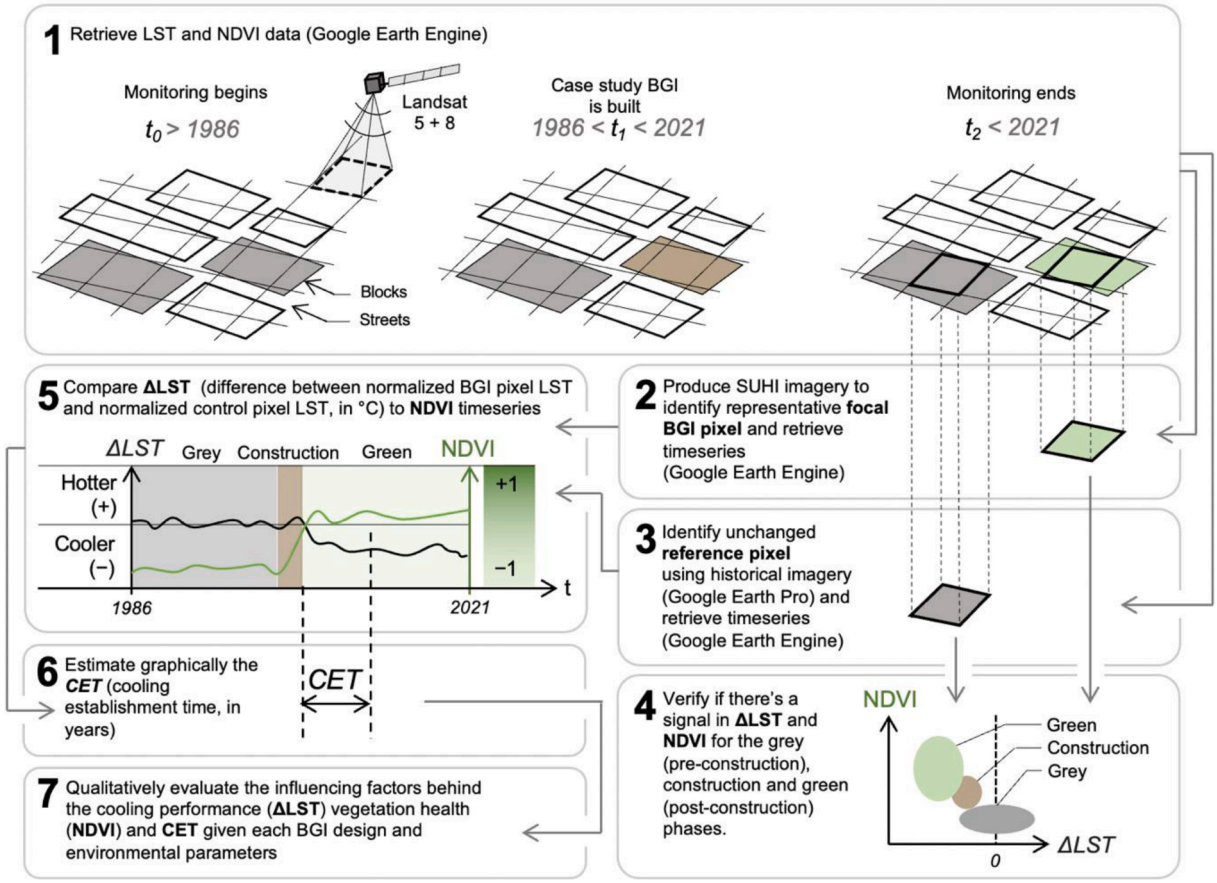

Fig. 1. Flowchart of methods involved in this research from data acquisition to establishment time results.

Table 1
Case studies used in this research. The icons illustrate pre-construction and post-construction situations and each case study is described by their construction date and approximate area (Stadt Zürich, 2023a).

		Site, Zurich district	Built in	Before	After	Aprox. Area [m^2]
	①	MFO-Park, Oerlikon	2001–2002	Industrial site	Metal structure vertical park	3300
	②	Hardaupark, Aussersihl	2011–2012	Parking lot	Park with scattered trees	7700
	③	Heinrichstrasse, Industriequartier	2005–2006	Industrial site	Building with an atrium	1800
	④	Wahlenpark, Seebach	2004–2005	Building	Grassland and trees	11,470
	⑤	Turbinenplatz, Escher Wyss	2003–2003	Industrial site	Paved square and vegetation	8500
	⑥	Tessinerplatz, Enge	2005–2006	Paved square	Square with trees	2030

high computational processing (Gorelick et al., 2017; Cossu et al., 2010; Nemani et al., 2011) we used the Google Earth Engine platform (Google Earth Engine, 2010). GEE is a cloud-based platform available via an application programming interface (API) that makes accessible the high-performance computing resources of Google's infrastructure (Fan et al., 2019). Satellite data catalogs are available within GEE with different levels of processing (Gorelick et al., 2017), including products from Landsat 5 and 8 satellite missions.

2.3. Spatio-temporal analysis of land surface temperature at each case study site

For each case study site an area of interest was defined to retrieve LST and NDVI time series from the satellite images. The area of interest corresponds to the shape of each BGI case study. This area can involve pixels that are fully within the BGI area, or involve pixels that are mixed between BGI and non-vegetated areas. If the area of interest involves more than one pixel, each of its resulting LST through time will be a weighted average between the sub-areas of the area of interest within each pixel. To decrease the influence of clouds, we discarded the pixels with more than 20% cloud cover over the whole image area.

However, as many other cities, Zurich presents a SUHI effect, as indicated in its recent Heat Mitigation Plan (Stadt Zürich, 2020) and which can be seen in detail in our supplementary materials. The construction site of each BGI is, hence, affected by this SUHI. This means that the LST time series of any satellite pixel within the urban areas of Zurich will tend to show a steady increase. Thus, in order to rule out influences of this overall urban temperature increase over time, we should not retrieve only the LST time series of the focal BGI pixel but we should retrieve also the LST time series of a reference pixel where land use has not changed during the course of the observation period. Within this surrounding pixel, any temperature increase should roughly

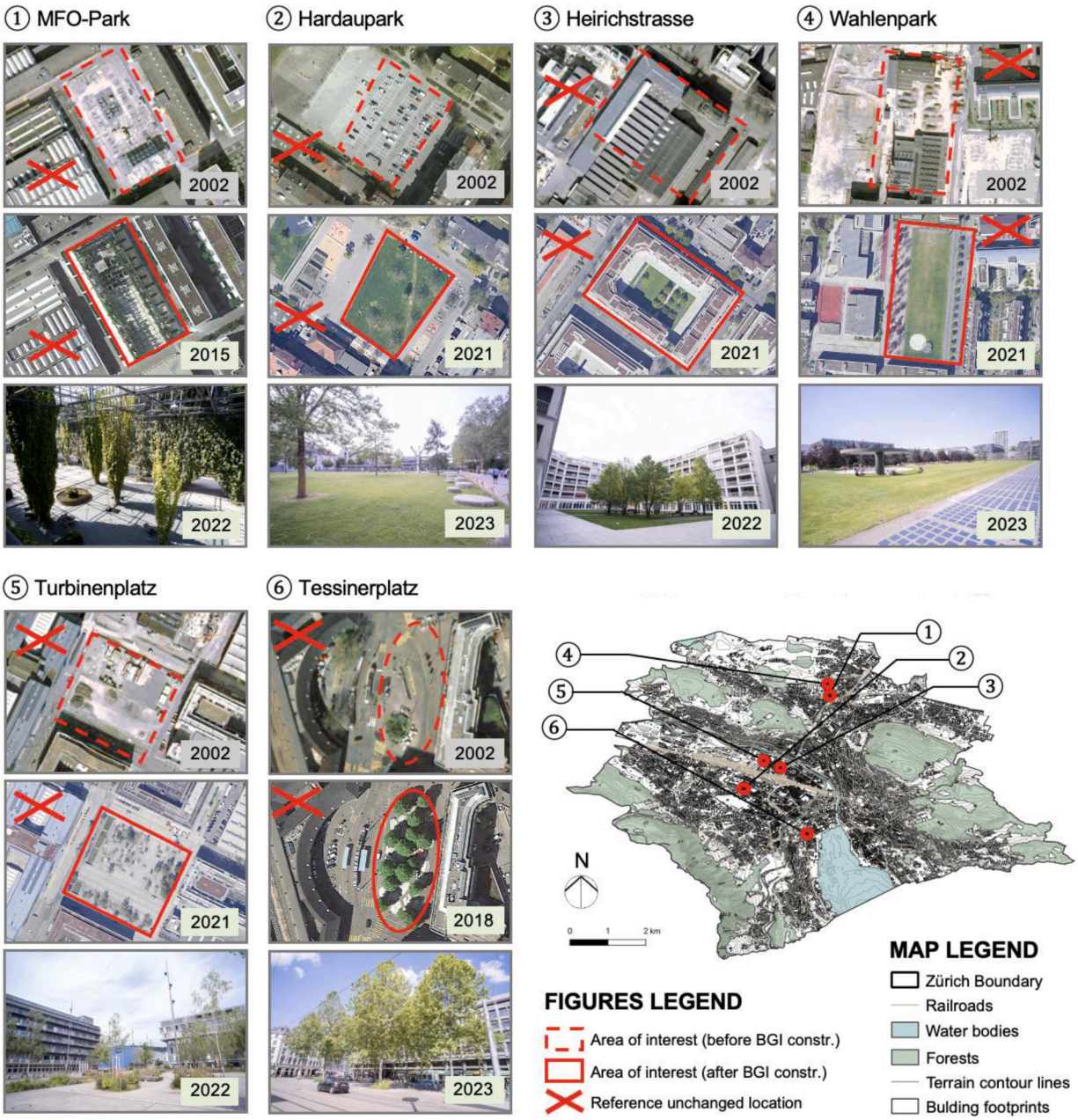

Fig. 2. Case study sites in the city of Zurich in Switzerland. Aerial imagery sourced from Google Earth Pro-and Geographical Information System data available at Stadt Zürich (2023b).

Table 2
Relevant parameters of each satellite product used in this research (ARSET, 2022; NASA, 2023; USGS, 2023).

Satellite	Sensors	Temporal coverage	Products	Passing time (local time)	Spatial resolution	Pixel size	Temporal resolution
Landsat 5	MSS and TM	03/1984 – 01/2013	LST and NDVI	10:00 am ± 15 min	120 m	30 m	16 days
Landsat 8	TIRS and OLI	02/2013 – Present	LST and NDVI	10:00 am ± 15 min	100 m	30 m	16 days

approximate the SUHI urban warming effect, given that no land use change has happened there. To this end, we produced not only a BGI focal pixel LST time series ($LST_{t,\ focal}$), but also an LST time series of a surrounding pixel ($LST_{t,ref}$), with t being the timestep related to the passing time of the Landsat missions where data were available and free of cloud influence.

This neighboring pixel was found using historical imagery from Google Earth Pro-and its LST time series derived using the same steps as for the focal BGI pixel (see description above). However, to generate a reference LST time series free from mean differences between the focal and reference pixels, we subtract the average temperature difference observed before the construction, where t^* represents the moment when construction starts and t' is a generic timestep:

$$LST_{t,ref,\ norm} = LST_{t,ref} - \left(\frac{1}{t^*} \sum_{t=0}^{t^*} LST_{t,ref} - \frac{1}{t^*} \sum_{t=0}^{t^*} LST_{t,\ focal} \right) \quad (1)$$

This ensures that the ΔLST (defined below) is centered around zero before the construction. Finally, a mean temperature difference of these two pixels is then calculated, making the BGI LST time-series now free from the SUHI effects, as seen in Eq. (2). This will produce finally a net relative mean LST time series of the focal BGI pixel relative to its surroundings, the ΔLST.

$$\Delta LST_t = LST_{t,\ focal} - LST_{t,ref,\ \ norm} \tag{2}$$

The final time-series produced is aggregated annually, for each of the N years, with each ΔLST point at N being the result of the average of all readings within that N-th year (Eq. (3)). The n_N is the number of ΔLST_t measured within that N-th year.

$$\Delta LST_N = \frac{1}{n_N}\sum_{N,t}\Delta LST_t\ ,\quad N \in\ \mathbb{Z},\quad N\subset[1985,\ 2021] \tag{3}$$

The process to retrieve the NDVI is slightly simpler, as it does not need to be compared to a surrounding pixel, it is retrieved from the focal pixel directly. The NDVI data is aggregated annually as the result of all readings in that N-th year (Eq. (4)).

$$NDVI_N = \frac{1}{n_N}\sum_{N,t}NDVI_{t,\ focal}\ ,\quad N \in\ \mathbb{Z},\quad N\subset[1985,\ 2021] \tag{4}$$

In some cases, the data is presented as a 2-year moving average to

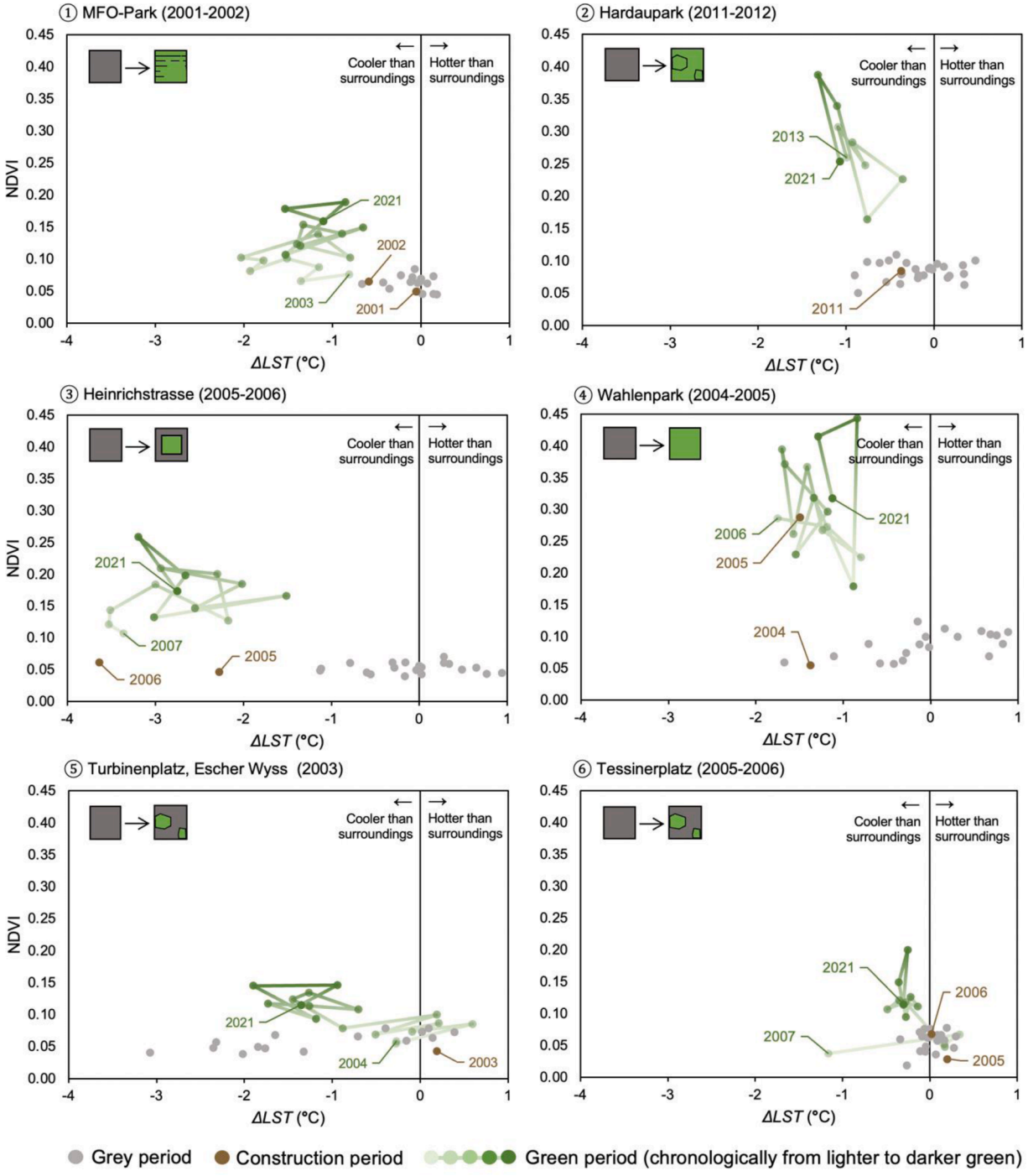

Fig. 3. Comparison between ΔLST and NDVI through time for each case study. Error bars represent the standard deviation from the mean.

make the visualization easier. During the construction period there will be vegetation added and after the BGI construction this vegetation will develop, increasing the BGI cooling effect. Over time, it is expected that a noticeable cooling effect will become visible and stabilize after some time, hence reaching the CET. The CET can be pinpointed graphically as the moment when a steadier LST state is achieved.

3. Results

3.1. Pre and post BGI construction differences

To investigate if satellite imagery can show a signal in LST and vegetation health comparing the pre-construction phase (gray period), construction phase and post-construction phase (green period), the annual scatter of NDVI vs. net relative mean temperature (ΔLST) is represented in Fig. 3. The objective of this figure is to demonstrate the relationship between ΔLST and NDVI. And as can be seen, as time progresses, NDVI increases tended to somewhat correlate with ΔLST decreases. We observed clustering when comparing the mean results from the gray to the scatter in the green period, showing a transition period that corresponds to the construction of the BGI.

The BGI in Heinrichstrasse (③), for example, showed the best outcomes in terms of LST reduction performance, reaching a maximum of 3.5 °C reduction when compared to its surrounding pixel. The worse maximum LST reduction was around 0.5 °C at Tessinerplatz (⑥). The case study with higher NDVI was Wahlenpark (④), reaching around

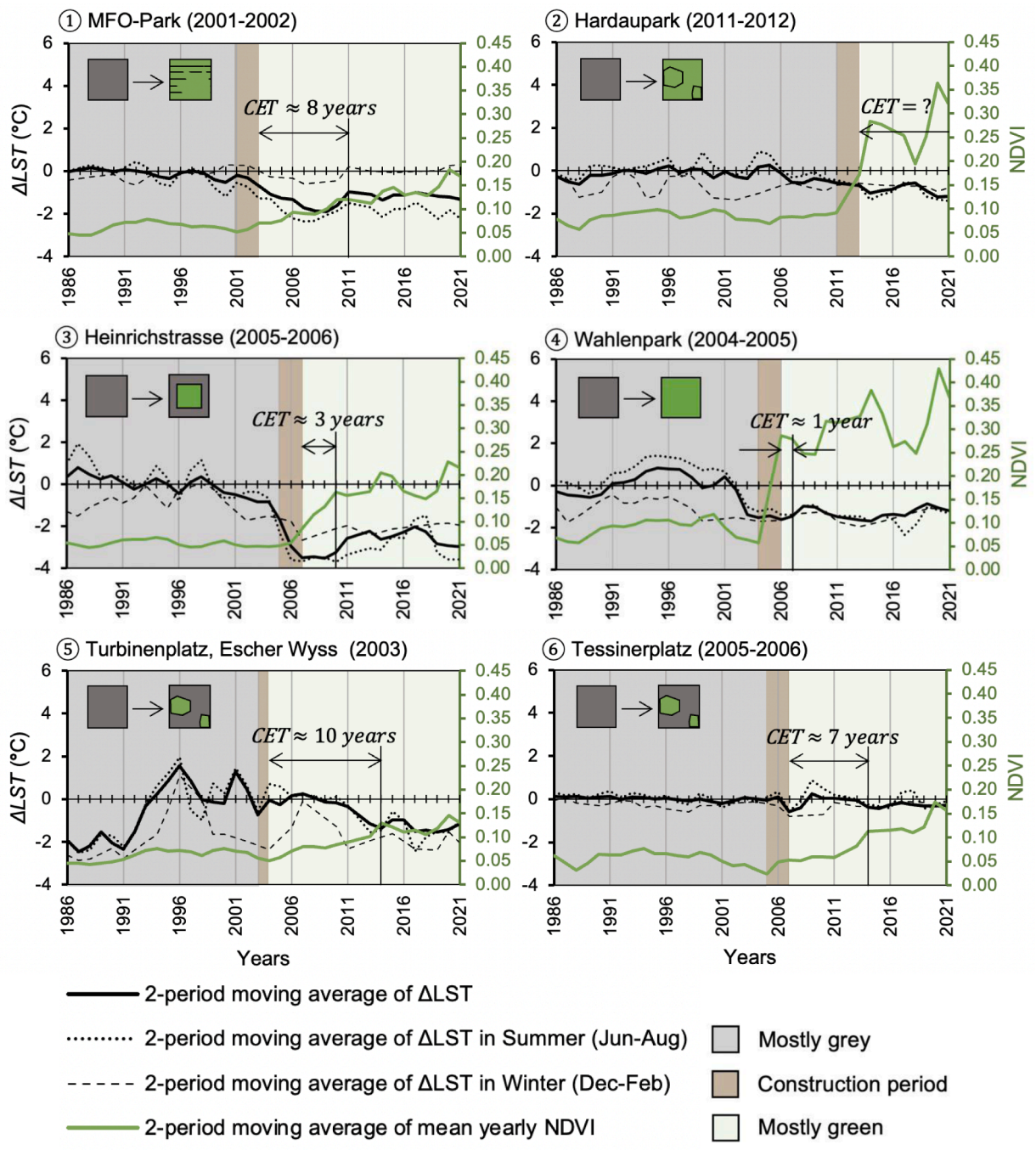

Fig. 4. Time series of ΔLST 2-year moving average (all year, only summer and only winter) and mean NDVI for each case study, using Landsat 5 and 8 data from 1985 to 2021.

+0.45. The worse NDVI performance was found in Tessinerplatz (⑥), where although LST cooling seems to have stagnated, the vegetation health explained by the NDVI has been increasing. Overall, Fig. 3 shows a negative correlation between the NDVI and the ΔLST. Despite this being an intuitive outcome in qualitative terms, quantifying this relation is a necessary intermediate step to show that there was a signal in LST difference when comparing the scenarios before and after the BGI implementation, that will support the later quantification of the time needed to reach this difference, or here the CET.

On top of that, the relationship between NDVI and ΔLST is different for each of these case studies. This can be explained by the fact that each case study represents a different BGI type. The vegetation health is not the sole factor explaining the cooling capacity of a BGI, but design factors and surrounding conditions are also relevant. Comparing the NDVI results to the common thresholds for vegetation health, it is possible to notice that all case studies surpassed the NDVI = +0.15 mark (Eastman et al., 2013) representing a natural arid environment, but not all of them reached the +0.50 < NDVI ≤ +1 interval (Hashim et al., 2019) representing low urban vegetation. This indicates that the NDVI can underestimate the overall vegetation health and development of a BGI, given that in some case studies the green coverage is scattered (such as in MFO-Park (①) and Tessinerplatz ⑥) in comparison to a fully plant covered parks (such as Hardaupark ② and Wahlenpark ④). Thus, absolute values of NDVI should be interpreted with care. None of the BGIs reached the +0.50 < NDVI ≤ +1 interval (Hashim et al., 2019) representing high urban vegetation, however the parks (Hardaupark ② and Wahlenpark ④) were close to reaching these NDVI values.

Another factor that can contribute to the different relationships between NDVI and ΔLST across different case studies is the view factor of the satellite, as mentioned before. The LST reductions provided by trees are happening mostly under the canopy and the satellite is capturing LST from the top of the canopy, which can create underestimations.

3.2. Cooling establishment time (CET)

The CET can be derived from the time series of ΔLST and NDVI. Thus, Fig. 4 shows temporal trends prior to, during and after BGI establishment for the six case studies. In every case, an inflection point is visible in the NDVI curve during the construction phase, most probably associated with the moment when built land cover is removed and vegetation is added. It is also clear that the NDVI increased during the post-construction period for all case studies. This increase in NDVI is explained by the growth and consolidation of plants (Nouri et al., 2017). As expected, as vegetation grows and establishes, the LST within the BGI (BGI focal pixel) goes down in relation to its surroundings.

Specific behaviors of ΔLST during the solstice seasons of the year are also noticeable in Fig. 4. During summer, when days are longer and temperatures higher, the temperature in the BGI areas before construction are similar than their surroundings. After the construction of the BGIs this pattern inverts. Summer temperatures in the BGI areas tend to be cooler than its surroundings; whereas in winter the net relative temperature in the BGI areas prior to and after its construction do not change significantly. A good example of this phenomena is Heinrichstrasse (③), where after the BGI construction the ΔLST during summer dropped substantially and winter ΔLST dropped less, inverting their positions. This can be explained by the high potential of vegetation to regulate energy exchange processes, meaning that the focal BGI pixel not necessarily got cooler in Summer, but did not heat up as much as their reference pixel. The case study with higher NDVI (Wahlenpark ④) had the shortest establishment time, mostly because the vegetation quickly developed to a higher maturity and, thus, it reached the maximum cooling performance faster.

The CETs observed in Fig. 4 for each of the case studies are heterogeneous. Some BGIs required around one to three years to reach the establishment level, whereas others seven or more years. This difference in CET is attributable to differences in vegetation development, which are a consequence of differences in maintenance, differences in environmental aspects or design aspects of the BGI.

4. Discussion

As demonstrated in previous studies, the use of satellite imagery is a powerful tool to assess the cooling capacities of urban greenery (Maimaitiyiming et al., 2014; Bartasaghi-Koc et al., 2019; Hami et al., 2019). Our study resonates with the results of these previous studies, as seen in the clear LST differences of the pre- and post-BGI construction. Furthermore, our investigation also confirmed the feasibility of using satellite imagery to derive BGI CETs. In the following sections, the association between the results found and design, environmental factors, vegetation and soil and water management are discussed. These are presented along with considerations about scaling this method for a larger quantitative analysis and the use of machine learning to support this process as well as the applicability of this research on a multi-criteria analysis and economic evaluation of BGIs. Specific limitations and further research are stressed in each section and general limitations are presented as a separate section.

4.1. Design and environmental factors

The different CETs as well as the different ΔLSTs found were a product of BGI designs, surrounding built environments, morphological and vegetation properties, which varied among the case studies. In terms of design properties, different areas, shapes and degrees of fragmentation were observed in the case studies. The low performance in terms of NDVI for Turbinenplatz (⑤) and Tessinerplatz (⑥) can, for example, be due to their multi-functional design intention: both are city squares with paved surfaces for pedestrian traffic and cultural events. This generated fragmentation (Cao et al., 2010), despite both having large areas and shapes that resemble squares and circular areas. As indicated by Wong et al. (2021) and Yu et al. (2017), regularly shaped green areas have been found to exhibit higher cooling performance, and this performance drops the more complex the shape is. All case studies considered in this study have regular shapes, however some, as indicated, have a more fragmented use of greenery over their areas.

Regarding surrounding built environment parameters, the CET and resulting ΔLSTs can also vary depending on the climate and microclimate where the case studies are located. In terms of climate, the Köppen-Geiger climate zone where the BGIs of our study are located (Cfa) is the second most studied in the world within the field of vegetation cooling research (Bartesaghi Koc et al., 2018). This points to the need to broaden the application of this method to other climate zones. In terms of microclimate, other authors have explored the influence of factors such as sky view factor, neighbouring buildings geometry, building shading, location relative to street orientation, distance to city center and relative wind speed and direction (Antoszewski et al., 2020). However, as the presented study analyses the temperature relative to surroundings, these effects should be mostly canceled out, and were not analysed. In any case, the City of Zurich has a very standardized maximum height allowance for buildings as well as similar street canyon aspect ratios. As such, the relative influence of these parameters among the BGIs considered in this study is likely to be low.

4.2. Vegetation

Conversely, vegetation properties may have played a greater role in the results observed. Longer CETs were found especially where the dominant vegetation, such as trees, takes longer to reach its maturity (Jaganmohan et al., 2016). Longer CETs, however, have not always resulted in a higher cooling performance, or higher ΔLST. As pointed out by Kong et al. (2014) and Feyisa, Dons & Meilby (2014), the type and species of dominant vegetation plays a role in the cooling capacity of a BGI. In terms of dominant vegetation as well as vegetation coverage

percentage, both Wahlenpark (④) and Hardaupark (②) used mostly grass. This created a high relative NDVI in comparison to the other case studies, but low ΔLST. Nevertheless, this also implies a lower CET as these plants take less time to establish, as could be seen in Fig. 4. Turbinenplatz (⑤) and Tessinerplatz (⑥) both took longer to reach their CET, given that there is a large use of trees instead of only grass and shrubs. MFO-Park (①) serves multiple functions, being a public site that provide space for congregation and shaded refuge from summer heat. The park is made of a steel structure with climbing plants, naturally taking time to slowly build up towards fully covered vertical greenery, thereby requiring a longer CET.

The use of native species and a high biodiversity tends to decrease the time needed for vegetation consolidation (Nagase & Dunnett, 2013), which has been the choice for most of the BGI analysed in our study. As pointed out by Leinster (2006), maintenance has great importance as well as the moment the vegetation is planted within the construction time period: depending on the need to finish other building phases in the construction site, vegetation can suffer damages, particularly in streetscape applications, delaying its establishment.

4.3. Soil and water management

Another important aspect is the occurrence of irrigation systems (Potchter et al., 2006). An artificial irrigation is found in Heinrichstrasse (③), a BGI within the courtyards of a building using mostly homogeneous grass and a few trees. The presence of irrigation facilitates the initial plant development and plant upkeep throughout drier seasons, which possibly influenced the CET, making it the shortest from the six BGI sites considered in this study. It was also observed that this irrigated BGI showed the best LST cooling performance, as seen by its ΔLST (Fig. 3).

The studies of Cao et al. (2010), Duncan (2019) and Du et al. (2017) explored the influence of soil, vegetation and impervious surface coverage percentage on BGI LST cooling performance, showing that larger pervious soil and vegetation coverage and less impervious surfaces yield better cooling performance. Other authors explored parameters such as plant density (e.g., Wang et al., 2015), vegetation structure, leeward vegetation coverage percentage, Leaf Area Index, soil hydration quality and synergistic effects with other BGIs in order to analyze the cooling performance of BGIs. We did not explore these parameters in our study, but including these parameters in further studies could yield interesting outcomes in terms of what are the main influencing factors on the CET.

4.4. Quantitative analysis and machine learning applications

Based on the results of our study, it was not possible to attribute to specific BGI properties the differences observed in ΔLST or CET. This would most likely require a much larger number of climate conditions and BGI properties to be considered. Our study presents a mostly qualitative insight into possible influence of environmental, design and maintenance characteristics that are likely to influence BGI CET. Whilst this provides an initial insight into understanding BGI establishment, the proposed methodology can be further improved through broader application to a wider range of case studies in order to also characterize the CET as a function of all parameters discussed above. This would identify the most sensitive parameters within the CET and assist in the planning, design, implementation and maintenance of BGI solutions.

This quantitative analysis with a wider range of case studies and parameters could be scaled up using with Machine Learning. Two main steps need to be automatized: (i) identification of place and time of construction of BGI in urban areas, and (ii) selection of suitable reference pixels without construction activities. Both lie within the realms of current image classifiers (Bhil et al., 2022). By these means, a large number of BGI's could be investigated, which would allow for statistical modeling of the CET as function of the environmental and design parameters presented in this article. As a sequence, to automatically and more accurately derive the CET, the work from Dalheim & Steen (2020) could be used, which proposes a steady state identifier model that can find stationary and non-stationary parts of time-series using a sliding window approach.

With the aid of Machine Learning approaches, this method could be not only scaled-up to more case studies withing the same climate, but also globally. This would make the evaluation of CET possible for a larger range of climate conditions at cities with also varying relevant urban parameters that could influence the establishment times.

4.5. Multi-criteria analysis and economic evaluation

To further enhance the understanding of factors influencing CET and their relative importance, results of a wider qualitative analysis can aid conducting a multi-criteria analysis. By employing this approach, the interactions and significance of various parameters can be systematically assessed, aiding in the prioritization of considerations during BGI planning and design. Multi-criteria analysis involves assigning weights to different criteria or parameters that influence CET, such as vegetation, design and environmental parameters. These weights reflect the relative importance of each factor in achieving the desired cooling outcomes. By assigning weights, decision-makers can quantify the importance of different parameters and incorporate them into a comprehensive evaluation framework and helping them guide the allocation of resources towards the most impactful aspects.

By conducting such analysis, it is possible to identify the most influential factors that significantly affect CET. For example, the analysis may reveal that vegetation type has a higher weight compared to geometrical properties, indicating that the choice of vegetation should be given more emphasis in BGI planning and design. This approach enables decision-makers to make informed choices based on a systematic and objective assessment of various factors.

Furthermore, multi-criteria analysis allows for the consideration of potential interactions between different parameters. For instance, it may reveal that certain combinations of vegetation type and irrigation systems yield more favourable CET outcomes than others. This insight can guide the selection of optimal BGI configurations that maximize cooling performance.

Specifically to CET, more accurately knowing how long different types of BGIs take to fully establish may assist in the right selection of BGI type to tackle urgent urban challenges. For example, areas where local population is experiencing heat vulnerability may need urban planners to act quickly. To that extent, choosing the right BGIs or vegetation to mitigate heat-related hazards in a timely manner involves balancing the cooling assets generated by these BGIs with their associated CETs.

In terms of economic evaluation, it is essential to consider the cost implications associated with different BGI design choices, maintenance requirements, and establishment times. The selection of vegetation types, irrigation systems, and geometrical properties can have varying financial implications. Conducting a cost-benefit analysis would provide insights into the long-term economic viability and return on investment of implementing BGIs with different CETs in diverse urban contexts, aligning budgetary constraints. By assessing the costs and benefits associated with BGI implementation, decision-makers can make informed choices regarding the most financially sustainable approaches. Such an analysis would consider not only the construction and maintenance costs but also assets such as the potential economic benefits derived from reduced energy consumption, improved air quality, enhanced property values, and health-related savings. By quantifying the economic advantages of BGIs over their lifecycle, decision-makers can make informed choices and prioritize investments in BGIs that yield the highest overall return on investment. This analysis would help prioritize cost-effective strategies that optimize the use of public funds.

4.6. General limitations and further work

The proposed analysis to estimate the CET of BGIs is limited by the spatial and temporal resolutions of the satellite imagery used. The use of remote sensing to evaluate the CET is constrained to the pixel size of the satellite imagery, given that BGIs smaller than the pixel size will have larger interference of the surrounding non-vegetated elements. Results are also constrained to the temporal resolution of the satellite sensors as well as the time span the data are available.

The view factor of the satellite imagery can also yield underestimations in the LST reduction or biases in the relationship between NDVI and ΔLST depending on the geometry of the vegetation. In the case of trees, for example, the greatest reduction in LST is happening under the tree canopy and not on top of the canopy which is where the satellite is mostly collecting data from. The passing time of the Landsat missions is also a limitation related to its view factor limitations: the satellite passes only at 10am, which means that the shadows and lights casted are being viewed by the satellite roughly at the same angle across its observations. Of course, with slight changes depending on the day of the year and latitude, given Earth's tilted rotation angle in relation to its translation around the Sun. To that extent, the satellite will only view an excerpt of the radiation dynamics along one day. This can generate biases if one wants to quantify the actual LST reduction effect, but as the objective of this work is to quantify the CET which is based in relative LST changes, the method is still robust.

Cloud coverage impacts also the applicability of the proposed methodology. Some climates present a large number of days covered by clouds throughout the year, such as the case of Zurich, which experiences frequent blankets of thick fog (Scherrer & Appenzeller, 2013). The advantages of using open-source satellite data (e.g., Landsat), are however significant, considering their free of charge as well as their data availability for the whole world, allowing reproducibility and broader global-scale analysis of different BGI CETs.

CET results found graphically must be interpreted with care, as the stabilization of cooling performance is slow and the boundaries between stable cooling or a still establishing cooling remain fuzzy. Increasing the number of case studies within the same classifications can yield more data and, thus, provide basis for a statistical analysis of CET.

5. Conclusions

Investigating the necessary time for BGI to reach a stable cooling capacity is a relevant matter for accurately estimating the dynamic cooling performance of these infrastructures. To that extent, we observed that:

- Satellite imagery combined with design and environmental factors can effectively estimate the Cooling Establishment Time (CET) of green infrastructure in urban areas based on their Land Surface Temperature (LST), providing insights into the dynamic cooling performance of BGIs.
- The CET of BGIs varies depending on factors such as vegetation type, design properties, surrounding built environment, and maintenance practices.
- BGIs with vegetation that takes longer to establish, such as trees and climbing plants, have higher CETs (around 7–10 years), while those with quicker consolidation, like grass, have lower CETs (around 1–3 years).
- Active irrigation systems could influence the CET outcomes, leading to shorter establishment times and improved cooling performance.

An accurate estimation of CET is crucial for assessing the dynamic cooling performance of BGIs and optimizing their placement in urban areas. In cities where urban heat islands and hotspots are progressively growing every year, having the tools to better estimate the outcomes of greenery planning is a foremost necessity. The main findings of this work point to the significance of future policies to consider the time it takes for BGIs to reach full maturity and, therefore, a stable cooling potential.

As main future directions outlined in the discussion that can rather improve the methodology proposed or apply the methods to a further explore deriving topics, we have that:

- There is a large potential in scaling up the proposed methodology, quantifying the BGIs CET and correlating these results to its influencing factors, a process which can be aided by using Machine Learning. This would largely enhance the generalizability of this study.
- The promising outcomes for the irrigated case study indicate that positioning BGIs in a city where there is naturally more runoff accumulation or underground water can also be a relevant topic of study to further explore the water availability correlation to the cooling capacity and CET.
- Economic evaluation and multi-criteria analysis of BGIs can be supported by the estimation of their CETs, being valuable tools for assessing the long-term economic viability, cost implications, and prioritization of different factors influencing CET, aiding decision-making in BGI planning, design and resource allocation.

Our methodology provides a useful approach for not only researchers that want to better understand the dynamics of BGI cooling over time, but also to decision-makers, who need to balance short-term retrofit and long-term solutions. To that extent, this study can support evidence-based urban greenery planning and design towards cooling our increasingly warming cities in a timely manner and in the locations where it is most required.

Declaration of Competing Interest

The authors declare that they have no known competing financial interests or personal relationships that could have appeared to influence the work reported in this paper.

Data availability

The data used is retrieved by a publicly available script from NASA-ARSET, which is referenced in the article.

Acknowledgments

This research was supported by the Swiss National Science Foundation "Heat-Down" project [grant number 200021_201029]. The authors thank the NASA Applied Remote Sensing Training (ARSET) and the support of Sean McCartney (NASA).

Supplementary materials

Supplementary material associated with this article can be found, in the online version, at doi:10.1016/j.scs.2023.104768.

References

ARSET. (2022). Satellite remote sensing for measuring urban heat islands and constructing heat vulnerability indices. NASA Applied Remote Sensing Training Program (ARSET). Available at: http://appliedsciences.nasa.gov/join-mission/training/english/arset-satellite-remote-sensing-measuring-urban-heat-islands-and.

Aflaki, A., Mirnezhad, M., Ghaffarianhoseini, A., Ghaffarianhoseini, A., Omrany, H., Wang, Z. H., et al. (2017). Urban heat island mitigation strategies: A state-of-the-art review on Kuala Lumpur, Singapore and Hong Kong. *Cities, 62*, 131–145. https://doi.org/10.1016/j.cities.2016.09.003

Akbari, H., & Kolokotsa, D. (2016). Three decades of urban heat islands and mitigation technologies research. *Energy and buildings, 133*, 834–842. https://doi.org/10.1016/j.enbuild.2016.09.067

Antoszewski, P., Świerk, D., & Krzyżaniak, M. (2020). Statistical review of quality parameters of blue-green infrastructure elements important in mitigating the effect of the urban heat island in the temperate climate (C) zone. *International Journal of Environmental Research and Public Health, 17*(19), 7093. https://doi.org/10.3390/ijerph17197093. MDPI AG.

Back, Y., Bach, P. M., Jasper-Tönnies, A., Rauch, W., & Kleidorfer, M. (2021). A rapid fine-scale approach to modelling urban bioclimatic conditions. *Science of The Total Environment, 756*. https://doi.org/10.1016/j.scitotenv.2020.143732

Bartesaghi Koc, C., Osmond, P., & Peters, A. (2018). Evaluating the cooling effects of green infrastructure: A systematic review of methods, indicators and data sources. *Solar energy, 166*, 486–508. https://doi.org/10.1016/j.solener.2018.03.008

Bartesaghi-Koc, C., Osmond, P., & Peters, A. (2019). Mapping and classifying green infrastructure typologies for climate-related studies based on remote sensing data. *Urban Forestry & Urban Greening, 37*, 154–167. https://doi.org/10.1016/j.ufug.2018.11.008

Bartesaghi-Koc, C., Osmond, P., & Peters, A. (2020). Quantifying the seasonal cooling capacity of 'green infrastructure types' (GITs): An approach to assess and mitigate surface urban heat island in Sydney, Australia. In *Landscape and urban planning, 203*. Elsevier BV, Article 103893. https://doi.org/10.1016/j.landurbplan.2020.103893

Beck, H., Zimmermann, N., McVicar, T., et al. (2018). Present and future Köppen-Geiger climate classification maps at 1-km resolution. *Scientific data, 5*, Article 180214. https://doi.org/10.1038/sdata.2018.214

Bhil, K., et al. (2022). Recent progress in object detection in satellite imagery: A review. In S. Aurelia, S. S. Hiremath, K. Subramanian, & S. K. Biswas (Eds.), *Sustainable advanced computing. lecture notes in electrical engineering*. Singapore: Springer. https://doi.org/10.1007/978-981-16-9012-9_18. vol 840.

Bowler, D. E., Buyung-Ali, L., Knight, T. M., & Pullin, A. S. (2010). Urban greening to cool towns and cities: A systematic review of the empirical evidence. *Landscape and urban planning, 97*(3), 147–155. https://doi.org/10.1016/j.landurbplan.2010.05.006

Cao, X., Onishi, A., Chen, J., & Imura, H. (2010). Quantifying the cool island intensity of urban parks using ASTER and IKONOS data. *Landscape and Urban Planning, 96*(4), 224–231. https://doi.org/10.1016/j.landurbplan.2010.03.008, 2010.

Cossu, R., Petitdidier, M., Linford, J., Badoux, V., Fusco, L., Gotab, B., et al. (2010). A roadmap for a dedicated earth science grid platform. *Earth Sci. Inf., 3*(3). https://doi.org/10.1007/s12145-010-0045-4

Dalheim, Ø.Ø., & Steen, S. (2020). A computationally efficient method for identification of steady state in time series data from ship monitoring. *Journal of Ocean Engineering and Science, 5*, 333–345. https://doi.org/10.1016/j.joes.2020.01.003

Deilami, K., Kamruzzaman, Md., & Liu, Y. (2018). Urban heat island effect: A systematic review of spatio-temporal factors, data, methods, and mitigation measures. *In International Journal of Applied Earth Observation and Geoinformation, 67*, 30–42. https://doi.org/10.1016/j.jag.2017.12.009. Elsevier BV.

Du, H., Cai, W., Xu, Y., Wang, Z., Wang, Y., & Cai, Y. (2017). Quantifying the cool island effects of urban green spaces using remote sensing Data. *Urban Forestry & Urban Greening, 27*, 24–31. https://doi.org/10.1016/j.ufug.2017.06.008

Duncan, J. M. A., Boruff, B., Saunders, A., Sun, Q., Hurley, J., & Amati, M. (2019). Turning down the heat: An enhanced understanding of the relationship between urban vegetation and surface temperature at the city scale. *Science of The Total Environment, 656*, 118–128. https://doi.org/10.1016/j.scitotenv.2018.11.223

Dutta, D., Kundu, A., Patel, N. R., Saha, S. K., & Siddiqui, A. R. (2015). Assessment of agricultural drought in Rajasthan (India) using remote sensing derived vegetation condition index (VCI) and standardized precipitation index (SPI). *The Egyptian Journal of Re- mote Sensing and Space Science, 18*, 53–63. https://doi.org/10.1016/j.ejrs.2015.03.006

Eastman, J. R., Sangermano, F., Machado, E. A., Rogan, J., & Anyamba, A. (2013). Global trends in seasonality of normalized difference vegetation index (NDVI), 1982–2011. *Remote Sensing, 5*, 4799–4818. https://doi.org/10.3390/rs5104799

Fan, H., Yu, Z., Yang, G., Liu, T. Y., Liu, T. Y., Hung, C. H., et al. (2019). How to cool hot-humid (Asian) cities with urban trees? An optimal landscape size perspective. *Agricultural and Forest Meteorology, 265*, 338–348. https://doi.org/10.1016/j.agrformet.2018.11.027

Fehmi, J. S., & Kong, T. M. (2012). Effects of soil type, rainfall, straw mulch, and fertilizer on semi-arid vegetation establishment, growth and diversity. *Ecological Engineering, 44*, 70–77. https://doi.org/10.1016/j.ecoleng.2012.04.014

Feyisa, G. L., Dons, K., & Meilby, H. (2014). Efficiency of parks in mitigating urban heat island effect: An example from Addis Ababa. *Landscape and Urban Planning, 123*, 87–95. https://doi.org/10.1016/j.landurbplan.2013.12.008

(GEE) Google Earth Engine. (2010) Available at https://earthengine.google.com/.

Ghofrani, Z., Sposito, V., & Faggian, R. (2017). A comprehensive review of blue-green infrastructure concepts. *International Journal of Environment and Sustainability, 6*(1), 15–36.

Gorelick, N., Hancher, M., Dixon, M., Ilyushchenko, S., Thau, D., & Moore, R. (2017). Google earth engine: Planetary-scale geospatial analysis for everyone. *Remote Sensing of Environment, 202*, 18–27. https://doi.org/10.1016/j.rse.2017.06.031

Grilo, F., Pinho, P., Aleixo, C., Catita, C., Silva, P., Lopes, N., et al. (2020). Using green to cool the grey: Modelling the cooling effect of green spaces with a high spatial resolution. In *Science of the total environment, 724*. Elsevier BV, Article 138182. https://doi.org/10.1016/j.scitotenv.2020.138182

Hami, A., Abdi, B., Zarehaghi, D., & Maulan, S. B. (2019). Assessing the thermal comfort effects of green spaces: A systematic review of methods, parameters, and plants' attributes. *Sustainable Cities and Society, 49*, Article 101634. https://doi.org/10.1016/j.scs.2019.101634

Hashim, H., Abd Latif, Z., & Adnan, N. A. (2019). Urban vegetation classification with NDVI threshold value method with very high resolution (VHR) pleiades imagery. *The International Archives of the Photogrammetry, Remote Sensing and Spatial Information Sciences, XLII-4/W16*, 237–240. https://doi.org/10.5194/isprs-archives-XLII-4-W16-237-2019

Howard, L. (1818). The climate of London, deduced from meteorological observations. In *Made at different places in the neighbourhood of the metropolis, 2* pp. 1818–1820). London: W. Phillips.

IPCC. (2022). Climate change 2022: Impacts, adaptation and vulnerability. Contribution of working group II to the sixth assessment report of the intergovernmental panel on climate change [H.-O. Pörtner, D.C. Roberts, M. Tignor, E.S. Poloczanska, K. Mintenbeck, A. Alegría, M. Craig, S. Langsdorf, S. Löschke, V. Möller, A. Okem, B. Rama (eds.)]. Cambridge University Press. Cambridge University Press, Cambridge, UK and New York, NY, USA, 3056, doi:10.1017/9781009325844.

Jaganmohan, M., Knapp, S., Buchmann, C. M., & Schwarz, N. (2016). The bigger, the better? The influence of urban green space design on cooling effects for residential areas. *Journal of Environmental Quality, 45*, 134–145. https://doi.org/10.2134/jeq2015.01.0062

Jamei, E., Ossen, D. R., Seyedmahmoudian, M., Sandanayake, M., Stojcevski, A., & Horan, B. (2020). Urban design parameters for heat mitigation in tropics. In *Renewable and sustainable energy reviews, 134*. Elsevier BV, Article 110362. https://doi.org/10.1016/j.rser.2020.110362

Jamei, E., Rajagopalan, P., Seyedmahmoudian, M., & Jamei, Y. (2016). Review on the impact of urban geometry and pedestrian level greening on outdoor thermal comfort. In *Renewable and sustainable energy reviews, 54* pp. 1002–1017). Elsevier BV. https://doi.org/10.1016/j.rser.2015.10.104

Jamei, Y., Rajagopalan, P., & Sun, Q., (Chayn) (2019). Spatial structure of surface urban heat island and its relationship with vegetation and built-up areas in Melbourne, Australia. In *Science of the total environment, 659* pp. 1335–1351). Elsevier BV. https://doi.org/10.1016/j.scitotenv.2018.12.308

Kaloustian, N., & Diab, Y. (2015). Effects of urbanization on the urban heat island in Beirut. In *Urban climate, 14* pp. 154–165). Elsevier BV. https://doi.org/10.1016/j.uclim.2015.06.004

Kim, J. P., & Guldmann, J. M. (2014). Land-use planning and the urban heat Island. In *Environment and planning B: Planning and design, 41* pp. 1077–1099). SAGE Publications. https://doi.org/10.1068/b130091p

Kong, F., Yin, H., James, P., Hutyra, L. R., & He, H. S. (2014). Effects of spatial pattern of greenspace on urban cooling in a large metropolitan area of eastern China. *Landscape and Urban Planning, 128*, 35–47. https://doi.org/10.1016/j.landurbplan.2014.04.018

Leinster, S. (2006). Delivering the final product - establishing vegetated water sensitive urban design systems. *Australasian Journal of Water Resources, 10*(3), 321–329. https://doi.org/10.1080/13241583.2006.11465295

Maimaitiyiming, M., Ghulam, A., Tiyip, T., Pla, F., Latorre-Carmona, P., Halik, Ü., et al. (2014). Effects of green space spatial pattern on land surface temperature: Implications for sustainable urban planning and climate change adaptation. *ISPRS Journal of Photogrammetry and Remote Sensing, 89*, 59–66. https://doi.org/10.1016/j.isprsjprs.2013.12.010

Mazer, G., Booth, D., & Ewing, K. (2011). Limitations to vegetation establishment and growth in biofiltration swales. *Ecological Engineering, 17*(4), 429–443. https://doi.org/10.1016/S0925-8574(00)00173-7

Monberg, R. J., Howe, A. G., Kepfer-Rojas, S., Ravn, H. P., & Jensen, M. B. (2019). Vegetation development in a stormwater management system designed to enhance ecological qualities. *Urban Forestry & Urban Greening, 46*, 12646. https://doi.org/10.1016/j.ufug.2019.126463

(NASA). (2023). National aeronautics and space administration. *Landsat Science*. Available at https://landsat.gsfc.nasa.gov/satellites/landsat-8/.

Nagase, A., & Dunnett, N. (2013). Establishment of an annual meadow on extensive green roofs in the UK. *Landscape and Urban Planning, 112*, 50–62. https://doi.org/10.1016/j.landurbplan.2012.12.007

Nemani, R., Votava, P., Michaelis, A., Melton, F., & Milesi, C. (2011). Collaborative supercomputing for global change science. *Eos Transactions American Geophysical Union, 92*(13), 109–110.

Nouri, H., Anderson, S., Sutton, P., Beecham, S., Nagler, P., Jarchow, C. J., et al. (2017). NDVI, scale invariance and the modifiable areal unit problem: An assessment of vegetation in the Adelaide Parklands. *Science of The Total Environment, 584–585*, 11–18. https://doi.org/10.1016/j.scitotenv.2017.01.130

Oke, T., Mills, G., Christen, A., & Voogt, J. (2017). *Urban climates*. Cambridge: Cambridge University Press. https://doi.org/10.1017/9781139016476

Oral, H. V., Carvalho, P., Gajewska, M., Ursino, N., Masi, F., Hullebusch, E. D.v., et al. (2020). A review of nature-based solutions for urban water management in European circular cities: A critical assessment based on case studies and literature. *Blue-Green Systems, 2*(1), 112–136. https://doi.org/10.2166/bgs.2020.932

Potchter, O., Cohen, P., & Bitan, A. (2006). Climatic behavior of various urban parks during hot and humid summer in the mediterranean city of Tel Aviv, Israel. *International Journal of Climatology, 26*, 1695–1711. https://doi.org/10.1002/joc.1330

Probst, N., Bach, P. M., LCook, L. M., Maurer, M., & Leitão, J. P. (2022). Blue Green Systems for urban heat mitigation: Mechanisms, effectiveness and research directions. *Blue-Green Systems, 1*(2), 348–376. https://doi.org/10.2166/bgs.2022.028, 4.

Rizwan, A. M., Dennis, L. Y. C., & Liu, C. (2008). A review on the generation, determination and mitigation of Urban Heat Island. *Journal of Environmental Sciences, 20*(1), 120–128. https://doi.org/10.1016/s1001-0742(08)60019-4

Santamouris, M. (2013). Using cool pavements as a mitigation strategy to fight urban heat island—A review of the actual developments. *Renewable and Sustainable Energy Reviews, 26*, 224–240. https://doi.org/10.1016/j.rser.2013.05.047

Santamouris, M., Synnefa, A., & Karlessi, T. (2011). Using advanced cool materials in the urban built environment to mitigate heat islands and improve thermal comfort

conditions. *Solar Energy, 85*(12), 3085–3102. https://doi.org/10.1016/j.solener.2010.12.023
Scherrer, S. C., & Appenzeller, C. (2013). Fog and low stratus over the Swiss Plateau – a climatological study. *International Journal of Climatology, 34*, 678–686. https://doi.org/10.1002/joc.3714
Stadt Zürich. (2023) Park- und Grünanlagen von A bis Z. Available at: https://www.stadt-zuerich.ch/ted/de/index/gsz/natur-erleben/park-und-gruenanlagen/parkanlagen-von-az.html.
Stadt Zürich. (2023) Geodaten. Available at: Https://www.stadt-zuerich.ch/ted/de/index/geoz/geodaten_u_plaene.html.
Sörensen, J., Persson, A., Sternudd, C., Aspegren, H., Nilsson, J., Nordström, J., et al. (2016). Re-thinking urban flood management – time for a regime shift. *Water, 8*(8), 332. https://doi.org/10.3390/w8080332
Stadt Zürich. (2020). *Fachplanung hitzeminderung.* Zürich.
(USGS) United States Geological Survey. (2023). Landsat missions. Available at https://www.usgs.gov/landsat-missions.
(US EPA) U. S. Environmental Protection Agency. (2016). *Heat island impacts. united states environmental agency*. Available at http://www.epa.gov/hiri/impacts/index.htm.
Vina, A., Gitelson, A. A., Nguy-Robertson, A. L., & Peng, Y. (2011). Comparison of different veg- etation indices for the remote assessment of green leaf area index of crops. *Remote Sensing of Environment, 115*, 3468–3478. https://doi.org/10.1016/j.rse.2011.08.010
Wang, Y., Bakker, F., de Groot, R., Wörtche, H., & Leemans, R. (2015). Effects of urban green infrastructure (UGI) on local outdoor microclimate during the growing season. *Environmental Monitoring and Assessment, 187*, 732. https://doi.org/10.1007/s10661-015-4943-2
Wong, N. H., Tan, C. L., Kolokotsa, D. D., & Takebayashi, H. (2021). Greenery as a mitigation and adaptation strategy to urban heat. *Nature Reviews Earth & Environment, 2*(3), 166–181. https://doi.org/10.1038/s43017-020-00129-5
Yang, J., Shi, Q., Menenti, M., Xie, Y., Wu, Z., Xu, Y., et al. (2022). Characterizing the thermal effects of vegetation on urban surface temperature. *Urban Climate, 44*, Article 101204. https://doi.org/10.1016/j.uclim.2022.101204
Yu, Z., Guo, X., Jørgensen, G., & Vejre, H. (2017). How can urban green spaces be planned for climate adaptation in subtropical cities? *Ecological Indicators, 82*, 152–162. https://doi.org/10.1016/j.ecolind.2017.07.002
Zhou, W., Wang, J., & Cadenasso, M. L. (2017). Effects of the spatial configuration of trees on urban heat mitigation: A comparative study. *Remote Sensing of Environment, 195*, 1–12. https://doi.org/10.1016/j.rse.2017.03.043